View metadata, citation and similar papers at core.ac.uk

brought to you by CORE

provided by Calhoun, Institutional Archive of the Naval Postgraduate School

Calhoun: The NPS Institutional Archive

Faculty and Researcher Publications | Faculty and Researcher Publications Collection

1974-12

Excitation of M1 and M2 states in (22)Ne by 180° electron scattering

Maruyama, X. K.

American Physical Society

Physical Review C, v. 10, no. 6, December 1974, pp. 2257-2264

http://hdl.handle.net/10945/47581

Calhoun is a project of the Dudley Knox Library at NPS, furthering the precepts and goals of open government and government transparency. All information contained herein has been approved for release by the NPS Public Affairs Officer.

Dudley Knox Library / Naval Postgraduate School
411 Dyer Road / 1 University Circle
Monterey, California USA 93943

http://www.nps.edu/library

Excitation of $M1$ and $M2$ states in ^{22}Ne by 180° electron scattering

X. K. Maruyama,* R. A. Lindgren,† W. L. Bendel, E. C. Jones, Jr., and L. W. Fagg
Nuclear Sciences Division, Naval Research Laboratory, Washington, D. C. 20375
(Received 22 May 1974; revised manuscript received 4 September 1974)

States in ^{22}Ne have been studied by 180° inelastic electron scattering with incident energies of 37, 50, and 60 MeV. Prominent magnetic dipole and quadrupole states are observed below 13 MeV excitation energy. Reduced transition probabilities, transition radii, and spin and parity assignments are presented for these states and compared to shell model calculations.

[NUCLEAR REACTIONS ^{22}Ne(e,e'), $E=37$, 50, and 60; measured $\sigma(E,180°)$; measured $B(M1)$; deduced J^π; enriched target.]

I. INTRODUCTION

Previous work using 180° inelastic electron scattering[1] has shown that strong $\Delta T=1$ magnetic dipole transitions occur in the $N=Z$ even-even sd shell nuclei. In ^{20}Ne,[2] ^{24}Mg,[3] and ^{28}Si[4] most of the $\Delta T=1$ $M1$ strength is concentrated in one or two levels. However, in the only $T_z=1$ nucleus studied, ^{26}Mg,[5] the $M1$ strength is fragmented over many levels. In order to study further the distribution of $M1$ strength in the $T_z=1$ nuclei, measurements were made on ^{22}Ne. Excitation energies and measured $M1$ strengths are compared to shell model calculations[6] which use the complete sd shell space, and the total strength is compared to the Kurath energy-weighted $M1$ sum rule.[7] These comparisons provide a stringent test of the shell model wave functions[8] and provide information on the relative importance of the spin-flip and the orbital recoupling components and on the distribution of the $M1$ strength as a whole.

As part of the program to systematically study magnetic transitions in the sd shell, we report here experimental results of electron scattering from ^{22}Ne at 37, 50, and 60 MeV. Excitation energies, spins and parities, transition strengths, and transition radii are extracted from the data.

II. GENERAL CONSIDERATIONS

A. Theory

The data are analyzed using the model-independent plane wave Born approximation (PWBA) expressions discussed by Rosen, Raphael, and Überall.[9] The corrections to the distorted wave Born approximation (DWBA) are obtained by using the tables of DWBA/PWBA of Chertok, Johnson, and Sarkar[10] for magnetic transitions and of Toepffer and Drechsel[11] for electric transitions. The tables of Toepffer and Drechsel are for the longitudinal part of the $E2$ interaction, not for the transverse part which dominates near 180°. However, they are judged to be more than sufficient for the accuracy of this work, particularly as the DWBA correction factors for $E1$ and $E2$ transitions are similar.

The cross section for inelastic magnetic scattering at 180° may be written[9]:

$$\frac{d\sigma}{d\Omega}=\frac{L+1}{L}\frac{\pi\alpha}{[(2L+1)!!]^2}\times B(ML,0)\uparrow\left(\frac{q^L G}{k_1}\right)^2\left(1+\frac{2\hbar c k_1}{M}\right)^{-1}, \quad (1)$$

where k_1 is the initial electron momentum in fm^{-1}, q is the momentum transfer in fm^{-1}, $\hbar c$ is 197.32 MeV fm, M is the atomic mass in MeV, α is the fine structure constant, and L is the multipolarity of the transition. $B(ML,0)\uparrow$ is the reduced transition probability from the ground to the excited state in units of fm^{2L}. The factor G contains the dependence on the transferred momentum and in the limit of low q is defined as

$$G(q,L,R)=\left[\frac{B(ML,q)}{B(ML,0)}\right]^{1/2}=1-\frac{L+3}{L+1}\frac{(qR)^2}{2(2L+3)}+\frac{L+5}{L+1}\frac{(qR^*)^4}{8(2L+3)(2L+5)}-\ldots . \quad (2)$$

The parameters R and R^* are transition radii as defined in Ref. 9. Although the interpretation of the radius R as a model-independent physical quantity is open to question, it has empirically been found to be approximately equal to the nuclear charge radius.[10] For the sd shell nuclei in the mass region $A=20$–28 previously studied in this laboratory[1] R has averaged slightly less than $1.0\,A^{1/3}$ fm for $M1$ transitions. As the R^* term is too small for experimental determination in the present work, we employ $R^*=R$.

The ground state radiative width of the transition is defined by

$$\Gamma_0 = \frac{L+1}{L}\frac{8\pi\omega}{[(2L+1)!!]^2}\left(\frac{\omega}{\hbar c}\right)^{2L} B(ML,\omega)\uparrow, \qquad (3)$$

where ω is the excitation energy in MeV. The $B\uparrow$ and $B\downarrow$ are related by

$$B(ML,\omega)\downarrow = \frac{2J_0+1}{2J+1} B(ML,\omega)\uparrow, \qquad (4)$$

where J_0 and J are the ground- and excited-state spins, respectively. Conventional units[12] for expressing $B(ML)$ are obtained by using the relationships $e^2 = 1.440$ MeV fm and $\mu_0{}^2 = 0.01589$ MeV/fm^3. Similar expressions for the electric transitions are found in Ref. 9.

B. Experiment

An electron beam of 1–4 μA, with full energy spread of 0.3%, from the Naval Research Laboratory 60 MeV electron linear accelerator was focused onto a cylindrical gas cell, 5.08 cm long and with end windows of 6 μm Havar. The cell contained ^{22}Ne, enriched to 99.5% isotopic purity, at 2.6 atm pressure and cooled to liquid nitrogen temperature. The scattered electrons are magnetically analyzed and are counted in one of 25 momentum bins formed by 13 overlapping scintillation counters in coincidence with a backing Cerenkov counter. Each channel in this system, patterned after the Amsterdam design,[13] observes a 0.28% momentum bite. A future publication will discuss the details of this detection system. The electron scattering facility is described more fully in a previous article[5] and the gas target cell has been described elsewhere.[14]

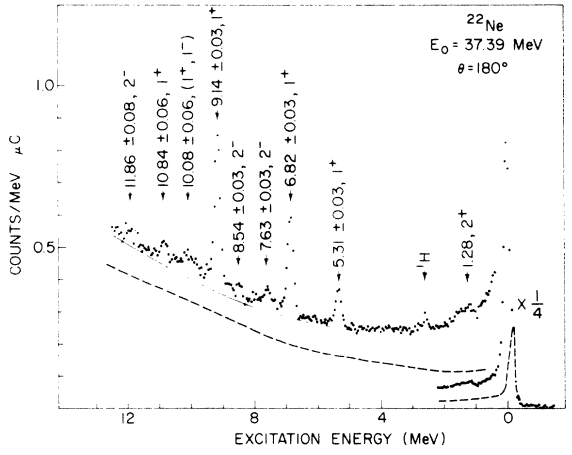

FIG. 1. Spectrum obtained by 180° scattering of 37.39 MeV electrons from ^{22}Ne. The solid line represents the assumed total background. The dashed line shows the spectrum obtained with an evacuated chamber. The spin and parities assignments of the observed states are determined from this experiment. Parenthesis indicate possible assignments. Level energies are in MeV. See text for details.

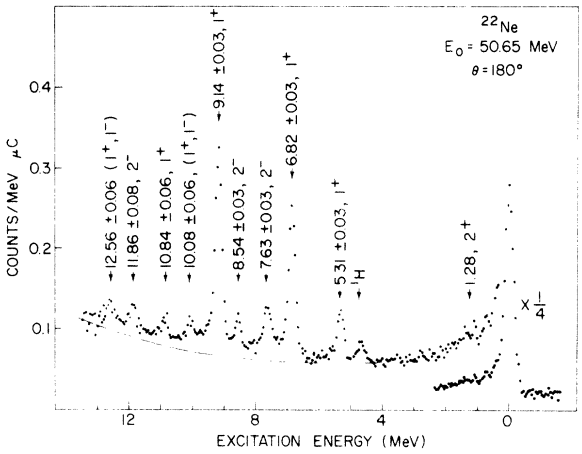

FIG. 2. Spectrum obtained by 180° scattering of 50.65 MeV electrons from ^{22}Ne. The solid line represents the assumed total background. Level energies are in MeV.

In general, the data are treated as in the previous works with appropriate corrections applied for ionization,[15] bremsstrahlung,[16] and Schwinger radiation[17] effects. Cross sections for ^{22}Ne are obtained by comparison to the hydrogen elastic peak[18] with 60 MeV incident energy electrons.

The errors given for the cross sections include counting statistics, uncertainties in the baseline, and line shape uncertainties in the case of overlapping levels. Additionally, a 10% error is assigned to the cross sections for ^{22}Ne to reflect normalization and instrumental uncertainties, such as density variations, molecular and isotopic impurities in the target, lack of knowledge of the ab-

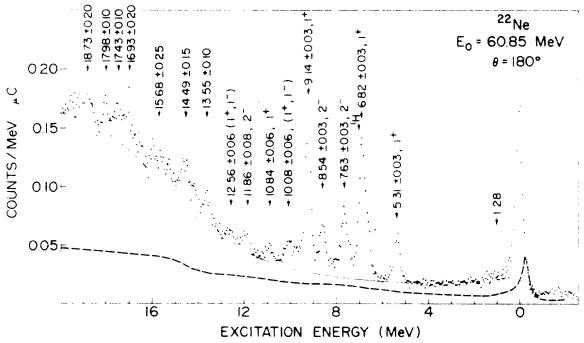

FIG. 3. Spectrum obtained by 180° scattering of 60.85 MeV electrons from ^{22}Ne. The solid line represents the assumed total background. The dashed line shows the spectrum obtained with an evacuated chamber. Level energies are in MeV.

solute proton cross section,[19] and reproducibility of standard cross sections in previous studies at this laboratory.

III. OBSERVED SPECTRA AND RESULTS

The spectra of electrons taken with incident energies of 37, 50, and 60 MeV are presented in Figs. 1, 2, and 3, respectively. Since detailed quantitative analyses of the spectra are confined to regions of excitation less than 13 MeV, only the 60 MeV data were taken to higher excitation energies. The spectra of electrons observed with an empty gas cylinder were taken at 37 and 60 MeV and are represented by the dashed lines in the figures. In both cases the target cell revealed no prominent features except for the elastic peaks due to the Havar-foil end windows.

As discussed in Ref. 2, the presence of the gas produces counts due to the gas and also alters the "background" in two significant respects. The electrons scattered at ~180° in the second Havar foil are degraded in energy by passing through the gas and the foil elastic peak will split into two peaks. In addition, small angle scattering in the gas will deflect electrons into the 1.11 cm diameter inner wall of the gas cell, producing counts by multiple scattering. It is seen, therefore, that a subtraction of the empty target cell spectrum from the ^{22}Ne spectrum does not yield the true net ^{22}Ne spectrum.

We have made calculations of the elastic radiative tail, but background contributions are dominant and the radiative tail calculations have not proved adequate to determining the "correct" total background to be used. Consequently, an empirical background curve is assumed as represented by the solid curves of Figs. 1, 2, and 3. The elastic radiative tail accounts for only 10 to 15% of the total observed background. For the 60 MeV data, the spectrum obtained from the empty target cell plus a constant equal to the observed spectrum above the elastic peak in addition to the calculated elastic tail proved to be coincident to the solid curve of Fig. 3 for excitation energies less than 12 MeV. For lower electron energies these attempts to explain the total background were less successful because multiple scattering effects cause a larger contribution to the spectrum. For example, accounting for the background as for the 60 MeV data, the 37 MeV spectrum exceeds the explained contributions by 20% at 3 MeV excitation and is too small by 7% at 12 MeV excitation energy.

Correction for a 0.5% hydrogen contaminant has been made in the 60 MeV analysis of the peak at 6.82 MeV excitation energy, where recoil has moved the hydrogen peak to the same excitation region.

Discrete peaks in ^{22}Ne are observed at 1.28, 5.31, 6.82, 7.63, 8.54, 9.14, 10.08, 10.84, and 11.86 MeV at all three bombarding energies. The state at 12.56 MeV was measured with 50 and 60 MeV incident electrons. Additional structure is observed with 60 MeV incident electrons at excitations of 13.55, 14.49, 15.68, 16.93, 17.43, 17.98, and 18.73 MeV. Table I lists the excitation energies and cross sections.

Where data are available at more than one incident energy, spin and parity determination of the observed levels have been made. For light nuclei[1] it is very improbable that transitions with $L>2$ would be observed with the momentum transfers in this experiment. In order to distinguish among $M1$, $M2$, $E1$, and $E2$ possibilities, the generalized Helm model[9] is employed. With reasonable values of transition radii, the model predicts the variation in cross section as a function of the incident energy. As the energy increases, the calculated values for $E1$ transitions decrease sharply; less sharply for the $M1$ and $E2$ cases; and are relatively constant for the $M2$'s. The states observed at 7.63, 8.54, and 11.86 MeV clearly have an $M2$ behavior. Only the states observed at 10.08 and 12.56 MeV have the possibility of being $E1$; an $E1$ assignment for the other states would require $R^2<0$. Transitions to the remaining states are consistent with $M1$ or $E2$.

Finally, theoretical considerations must be invoked to exclude the possibility that the observed transitions are $E2$ since electron scattering at 180°

TABLE I. Values of differential cross sections for states observed in this experiment in units of 10^{-32} cm^2/sr. The incident electron energies are 37.39, 50.65, and 60.85 MeV.

Excitation energy (MeV)	$(d\sigma/d\Omega)_{37}$	$(d\sigma/d\Omega)_{50}$	$(d\sigma/d\Omega)_{60}$
1.27 ± 0.15	≤0.16	≤0.14	≤0.020
5.31 ± 0.03	0.268 ± 0.033	0.185 ± 0.020	0.109 ± 0.012
6.82 ± 0.03	0.640 ± 0.069	0.510 ± 0.053	0.337 ± 0.034
7.63 ± 0.03	0.191 ± 0.029	0.209 ± 0.024	0.171 ± 0.021
8.54 ± 0.03	≤0.19	0.116 ± 0.015	0.127 ± 0.017
9.14 ± 0.03	0.992 ± 0.103	0.607 ± 0.062	0.326 ± 0.035
10.08 ± 0.08	0.257 ± 0.036	0.107 ± 0.016	0.068 ± 0.011
10.84 ± 0.06	0.134 ± 0.028	0.092 ± 0.012	0.039 ± 0.008
11.86 ± 0.08	0.097 ± 0.030	0.107 ± 0.016	0.072 ± 0.010
12.56 ± 0.06		0.087 ± 0.017	0.040 ± 0.009
13.55 ± 0.10			0.029 ± 0.009
14.49 ± 0.15			0.163 ± 0.020
15.68 ± 0.25			0.068 ± 0.015
16.93 ± 0.20			
17.43 ± 0.10			0.157 ± 0.024
17.98 ± 0.08			
18.73 ± 0.20			0.112 ± 0.018

TABLE II. Reduced matrix element extracted from fitting the data assuming an electric quadrupole transition.

Level energy (MeV)	$B(E2)\downarrow$ (e^2 fm^4)
5.31 ± 0.03	22.9 ± 5.6
6.82 ± 0.03	32.0 ± 6.2
9.14 ± 0.03	38.2 ± 4.9
10.08 ± 0.08	$8.0^{+1.6}_{-0.9}$
10.84 ± 0.06	3.5 ± 0.9
12.56 ± 0.06	$3.0^{+1.9}_{-1.4}$

with the energies of this experiment is incapable of distinguishing between $M1$ and $E2$ transitions. Table II presents values of the reduced matrix element to the ground state if an electric quadrupole transition is assumed. Shell model calculations for states above 6 MeV excitation in ^{22}Ne show that $E2$ transitions to the ground state are weak, and it is extremely unlikely that $B(E2)\downarrow \geq 3e^2\,\mathrm{fm}^4$. For all the states in our study, we conclude that the assumption of an $E2$ transition leads to unreasonably large reduced matrix elements. However, weak $E2$ transitions to states, which would be unresolved from the strong $M1$ states, could be present.

The results of this analysis are summarized in Table III. Of the nine states quantitatively analyzed, three states (7.63, 8.54, and 11.86 MeV) have $J^\pi = 2^-$, four states (5.31, 6.82, 9.14, 10.84 MeV) have distinctly 1^+ character, and two states (10.08 and 12.56 MeV) are compatible with either $J^\pi = 1^+$ or 1^-.

IV. DISCUSSION

In ^{22}Ne, the lowest $T=2$ state, which would be the analog of the ^{22}F ground state, is expected to be near 14 MeV excitation.[20,21] For states below this excitation energy, it is assumed that the isospin is $T=1$.

Comparison to other experiments

Many reactions[21-29] have been studied to extract spectroscopic information on ^{22}Ne. The resolution available in the present experiment is insufficient to rule out the possibility of exciting both members of doublet states in the region of interest. Table IV presents states observed in other experiments which are candidates for identification with the states observed in (e, e'). Arguments are presented below to identify the states observed in this experiment with those seen in previous works.

1.28 MeV. The well known 2^+ state[21] at 1.275 MeV is observed in 180° electron scattering as weakly excited. The quality of the data is insufficient to extract cross sections in the present experiment.

5.31 MeV. Silbert and Jaramie[22] observed a strongly excited state at 5.34 MeV using the ^{20}Ne$(t,p)^{22}$Ne reaction. This state may be identified with the 2^+ state at 5.360 MeV observed in other reactions.[24,25,23] The (d,p) and (t,α) reactions also note the existence of a state at 5.335 MeV with

TABLE III. Summary of results of this experiment showing excitation energy, spin and parity, transition radius, reduced matrix elements, electromagnetic width to the ground state, and transition strength. The Weisskopf unit is defined in Ref. 12. Where two J^π assignments are made, the data are compatible with either designation.

Level energy (MeV)	J^π	R (fm)	$B(\lambda L)\downarrow$ (e^2 fm^{2L} or μ_0^2 fm^{2L-2})	Γ_0 (eV)	Transition strength (Weisskopf units)
5.31 ± 0.03	1^+	$2.51^{+0.18}_{-0.31}$	0.074 ± 0.013	0.127 ± 0.022	0.040 ± 0.007
6.82 ± 0.03	1^+	$2.24^{+0.24}_{-0.42}$	0.166 ± 0.026	0.611 ± 0.096	0.092 ± 0.014
9.14 ± 0.03	1^+	$2.85^{+0.11}_{-0.14}$	0.320 ± 0.030	2.83 ± 0.26	0.176 ± 0.016
10.84 ± 0.06	1^+	$2.86^{+0.25}_{-0.30}$	$0.045^{+0.016}_{-0.012}$	$0.66^{+0.24}_{-0.17}$	$0.025^{+0.009}_{-0.006}$
10.08 ± 0.03	1^+	$3.15^{+0.15}_{-0.19}$	0.095 ± 0.016	1.13 ± 0.14	0.042 ± 0.007
	1^-	$1.89^{+0.64}_{-1.89}$	$0.031^{+0.009}_{-0.007}$	33^{+10}_{-7}	$0.061^{+0.017}_{-0.014}$
12.56 ± 0.06	1^+	$3.14^{+0.32}_{-0.66}$	$0.058^{+0.037}_{-0.028}$	$1.34^{+0.86}_{-0.65}$	$0.032^{+0.021}_{-0.016}$
	1^-	$2.60^{+0.51}_{-2.60}$	$0.21^{+0.013}_{-0.008}$	44^{+28}_{-17}	$0.042^{+0.026}_{-0.016}$
7.63 ± 0.03	2^-	3.69 ± 0.30	$10.1^{+2.5}_{-2.3}$	$(2.34^{+0.58}_{-0.51}) \times 10^{-3}$	$0.78^{+0.19}_{-0.17}$
8.54 ± 0.03	2^-	$3.07^{+0.53}_{-1.10}$	$3.5^{+2.1}_{-1.2}$	$(1.46^{+0.87}_{-0.49}) \times 10^{-3}$	$0.27^{+0.16}_{-0.09}$
11.86 ± 0.08	2^-	$4.10^{+0.26}_{-0.59}$	$6.9^{+2.9}_{-2.4}$	$(1.43^{+0.60}_{-0.49}) \times 10^{-3}$	$0.52^{+0.22}_{-0.18}$

TABLE IV. Excitation energies (MeV) and spin and parity of states observed in the present experiment, compared with states observed in other experiments.

Present work, level energy, and J^π	(t,p) [a]	(d,p) [b]	(^{7}Li,t) [c]	(t,α) [d]	Currently-accepted [e] level energy and J^π
1.27 ± 0.15					1.275 2^+
5.31 ± 0.03 1^+		5.331		5.350	5.335 ± 0.009 $(1,2)^+$
	5.340	5.359	5.370	5.360	5.360 ± 0.008 2^+
	6.823	6.821	6.820	6.800	6.819 ± 0.007 2^+
6.82 ± 0.03 1^+	6.860	6.858		6.840	6.855 ± 0.008 $(1,2)^+$
	7.633	7.630	7.640		7.632 ± 0.008 $(1,2)^+$
7.63 ± 0.03 2^-	7.663	7.658			7.660 ± 0.008 $(0-3)^-$
8.54 ± 0.03 2^-		8.548			8.548 ± 0.010 $(0-4)^+$
	8.575	8.585	8.590		8.583 ± 0.008 $(1,2)^+$
9.14 ± 0.03 1^+	9.174				9.174 ± 0.015
	$(\alpha,\eta\gamma)$ [f]	(α,α) [g]	$(t,^3\mathrm{He})$ [h]		Currently-accepted [e] level energy and J^π
	11.745				11.75 ± 0.01
	11.751	11.76			11.76 ± 0.01 1^-
11.86 ± 0.08 2^-	11.89	11.89			11.89 ± 0.01 1^-
					11.92 ± 0.01 (2^+)
		12.48			12.48 ± 0.01 (2^+)
12.56 ± 0.06 $(1^+,1^-)$		12.58			12.58 ± 0.01 (1^-)
		12.61			12.61 ± 0.01 $(1^-,2^+)$
15.68 ± 0.25			15.400 ± 0.040, $T=2$		
			15.610 ± 0.060, $T=2$		

[a] ^{20}Ne$(t,p)^{22}$Ne, Ref. 22.
[b] ^{21}Ne$(d,p)^{22}$Ne, Ref. 24.
[c] ^{18}O(^{7}Li,t)^{22}Ne, Ref. 25.
[d] ^{23}Na$(t,\alpha)^{22}$Ne, Ref. 23.
[e] Reference 21.
[f] ^{18}O$(\alpha,\eta\gamma)^{21}$Ne, Ref. 27.
[g] ^{18}O$(\alpha,\alpha)^{18}$O, Ref. 28.
[h] ^{22}Ne$(t,^3\mathrm{He})^{22}$F, Ref. 20.

either 1^+ or 2^+ character. The momentum transfer dependence observed at 5.3 MeV is uniquely that of an $M1$ transition. A 2^+ state of reasonable strength would not be observed in the present experiment. Therefore, the state we observe must be the lower member of the doublet, and its spin and parity are unambiguously $J^\pi = 1^+$.

6.82 MeV. The (t,p),[22] (d,p),[24] (^{7}Li, t)[25] and (t,α)[23] reactions show a 2^+ state at 6.819 MeV and a second member of the doublet is seen at 6.855 MeV in the (t,p), (d,p), and (t,α) reaction with tentative $J^\pi = (1,2)^+$. However, since (t,p) only weakly excites this state, the higher-energy member of the doublet could have unnatural parity. We identify the level at 6.855 MeV with the 6.82 MeV level in this experiment and conclude that $J^\pi = 1^+$. However, as shown in Table III, the transition radius for this state is smaller than for the other 1^+ states, so it is possible that there is some contribution from the lower-energy 2^+ state to the electron scattering cross section.

7.63 MeV. A doublet at 7.632 and 7.660 with uncertain spin and parity assignments of $(1,2)^+$ and $(0-3)^-$, respectively, has been observed in the (t,p) and (d,p) reactions. Only the lower-energy state is seen with (^{7}Li, t) and the higher-energy state is only weakly excited via (t,p). In the present experiment, we observe a 2^- state in this region which we identify with the negative parity 7.660 MeV state and remove the spin uncertainty.

8.54 MeV. The (d,p) reaction excites the lower member of the doublet at 8.548 MeV with tentative designations $J^\pi = (0-4)^+$. The (t,p), (d,p), and (^{7}Li, t) reactions all show the 8.583 MeV state of uncertain $J^\pi = (1,2)^+$. The 2^- state observed in electron scattering is identified with the 8.548-MeV state as one would not expect to easily observe an unnatural parity state with (t,p). The electron scattering analysis, however, disagrees with the previous tentative positive parity assignment.

9.14 MeV. Previously, only the ^{20}Ne$(t,p)^{22}$Ne experiment has explored this region of the ^{22}Ne spectrum. A weak state is seen at 9.174 MeV in the (t,p) reaction. Since it is weak, it is consistent that it may be the same 1^+ state we see at 9.14 MeV.

States >10 MeV excitation. Although states near 11.86, 12.56, and 15.68 MeV have been observed in reaction experiments,[20,27,28] it is difficult to make positive identification of these states with the levels observed in electron scattering. The peaks

TABLE V. States of $J^\pi = 1^+$ and reduced matrix elements to ground state from shell model calculations (Ref. 12) compared with experiment.

Level energy (MeV)	Theory $B(M1)$ (μ_0^2)	Candidate states from present exp.	Experiment $B(M1)$ (μ_0^2)
1_1 5.03	0.0411	5.31 ± 0.03	0.074 ± 0.013
1_2 6.48	0.338	6.82 ± 0.03	0.166 ± 0.026
1_3 8.24	0.0902	10.08 ± 0.08	0.095 ± 0.016
1_4 8.82	0.737	9.14 ± 0.03	0.320 ± 0.030
1_5 9.84	0.001 89	Below exp sensitivity	
1_6 10.55	0.151	10.84 ± 0.06	$0.045^{+0.016}_{-0.012}$
1_7 11.44	0.001 99	Below exp sensitivity	
1_8 12.00	0.0275	12.56 ± 0.06	$0.058^{+0.037}_{-0.028}$

observed in the present experiment above 10 MeV excitation energy are not as prominent as those at lower energies. Table IV summarizes this situation.

Comparison with the shell model

Preedom and Wildenthal[6,8] have performed an extensive shell model study of ^{22}Ne using the Oak Ridge-Rochester shell model codes.[29,30] This shell model calculation assumes an inert ^{16}O core with six particles in the sd shell. Their calculation employs the single particle energies from ^{17}O and an empirically modified Kuo interaction[31] which yields the best rms fit to 72 energy levels in the $A = 18$–22 mass region.

In the region of investigation of the present experiment, Preedom and Wildenthal predict eight $J^\pi = 1^+$ states. These are presented in Table V and Fig. 4. Of these eight 1^+ states, two have reduced matrix elements too small to be observable in this experiment. The six relatively strong 1^+ states coincide quite nicely with the six possible 1^+ states observed here. The predicted $M1$ strength is concentrated between 5 and 10 MeV, agreeing with the experimental evidence. However, on a quantitative basis the shell model predicts transition strengths which are, in general, too large. The calculated sum of $B(M1)\downarrow$ is $1.39\mu_0^2$ in contrast to the possible experimental value of $(0.76 \pm 0.12)\mu_0^2$. Note that the 10.08 MeV state is assigned to 1_3. On the whole, the agreement between experiment and theory is surprisingly good, especially when considering how sensitive the $M1$ widths are to admixed configurations.

Comparison with the $M1$ sum rule

It is useful to apply the Kurath energy-weighted sum rule[7] to ^{22}Ne to see how much of the available $M1$ strength is concentrated in the observed levels. The sum rule can be written[32] as

$$4\pi \sum_i E_i B_i(M1)\downarrow \simeq -a(\mu_n - \mu_p + \tfrac{1}{2})^2 \left\langle 0 \left| \sum_k \vec{l}_k \cdot \vec{s}_k \right| 0 \right\rangle \tag{5}$$

and

$$\left\langle 0 \left| \sum_k \vec{l}_k \cdot \vec{s}_k \right| 0 \right\rangle = \tfrac{1}{2}[l\langle n_{l+1/2}\rangle - (l+1)\langle n_{l-1/2}\rangle], \tag{6}$$

where $\langle n_{l+1/2}\rangle$ and $\langle n_{l-1/2}\rangle$ are the occupation numbers for the $d_{5/2}$ and $d_{3/2}$ orbits in the ^{22}Ne ground state. $B_i(M1)\downarrow$ is the reduced $M1$ transition probability in units of squared nuclear magnetons (μ_0^2), "a" is the spin-orbit strength derived from the $d_{5/2}$ and $d_{3/2}$ splitting in ^{17}O, and μ_n and μ_p are the neutron and proton magnetic moments, 2.79 μ_0 and −1.91 μ_0, respectively.

The sum rule is approximate since the isoscalar part of the magnetic dipole operator is neglected and it is assumed that the noncommutability of the $M1$ operator with the tensor, spin, or velocity-dependent terms in the Hamiltonian adds a small correction to the Kurath sum rule. The calculated isoscalar shell model matrix elements are less than 5% of the isovector and consequently can be neglected. However, neglect of the tensor terms in the Hamiltonian may be more significant. To get an estimate of how significant this may be in ^{22}Ne, one can use the shell model calculations previously described to evaluate the right-hand side (RHS) of Eq. (5). Using occupation numbers of $\langle d_{5/2}\rangle = 4.60$ and $\langle d_{3/2}\rangle = 0.66$ from Wildenthal,[8] and with $a = -2.0$ MeV, the RHS of Eq. (5) is 127 MeV μ_0^2. There are eight strong $M1$ transitions

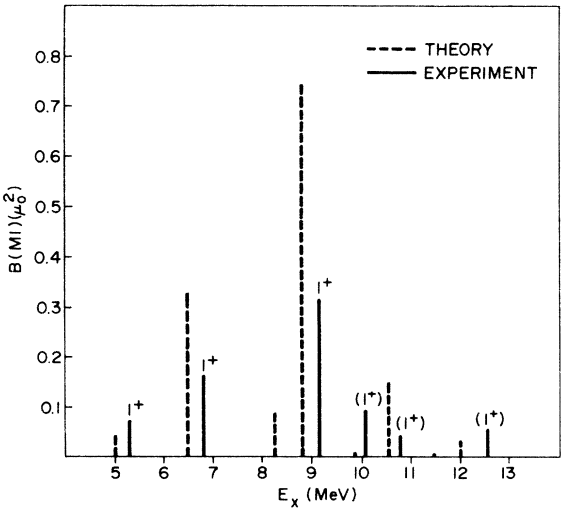

FIG. 4. Comparison of measured and calculated $M1$ strength for $J^\pi = 1^+$ states in ^{22}Ne.

TABLE VI. Comparison of total measured $M1$ strength with the energy-weighted $M1$ sum rule prediction.

Nucleus	$61.35\sum_i \Gamma_{i/E_i}{}^2$	$-a\langle 0\vert\sum_k \vec{l}_k\cdot\vec{s}_k\vert 0\rangle$ [a] (b)	(c)
^{20}Ne	5.45	8.0	3.14
^{22}Ne	4.68	12.0	8.24
^{24}Mg	14.1	16.0	
^{26}Mg	19.6	20.0	
^{28}Si	18.8	24.0	

[a] Value for a is -2.0 MeV.

[b] Calculated in the independent single-particle model.

[c] Occupation numbers calculated from the *sd* shell model (Ref. 8).

that are calculated in ^{22}Ne. Using these eight, which are shown in Table V, the LHS of Eq. (5) becomes 145 MeV $\mu_0{}^2$, a value 14% larger than the RHS. Consequently, the omitted terms would contribute at least 14% to the RHS of the sum rule. Summing the measured $M1$ transitions in Table V, the LHS becomes 83 MeV $\mu_0{}^2$, which is more than half of the limit 145 MeV $\mu_0{}^2$ calculated with the shell model wave functions.

Another way of writing the $M1$ sum rule is

$$61.35\sum_i \frac{\Gamma_i(\mathrm{eV})}{E_i{}^2(\mathrm{MeV})} \simeq -a\left\langle 0\left|\sum_k \vec{l}_k\cdot\vec{s}_k\right|0\right\rangle, \quad (7)$$

where Γ_i is the radiative width in eV and E_i is the excitative energy in MeV. This form has been used to apply the sum rule to nuclei near ^{22}Ne, with results shown in Table VI. The trend of the energy-weighted sum through the *sd* shell follows the single particle shell model predictions leading to maximum strength in nuclei where the $d_{5/2}$ orbit is filled. Apart from the approximate validity of the sum rule as previously mentioned and the uncertainties in the measurements, a large part of the departure from the single-particle limit is probably due to increased amplitude of the $d_{3/2}$ orbit in the ground-state wave function. In ^{20}Ne and ^{22}Ne, where ground state wave functions have been calculated in the complete *sd* shell space, the RHS of Eq. (7) are 3.14 and 8.24, respectively, which are smaller than the single particle limit (see Table VI) and closer to experiment.

In ^{22}Ne the largest contribution to the sum rule is the $M1$ transition to the 9.14 MeV level (see Fig. 4). Inspection of the components of the calculated transition (8.82 MeV), which consists of a large number of interfering matrix elements, shows that it is approximately half spin-flip and half orbital.

The calculated $M1$ transitions to levels below 8.82 MeV (see Table V) are dominated by orbital components. The strong $M1$ transitions to levels above 8.82 MeV are dominated by spin-flip. This is because the higher-lying excited states have increasingly more $d_{3/2}$ strength than the lower excited states. Both orbital and spin-flip components are contributing to the transitions and this results in a spreading of the strength over a number of levels.

In ^{20}Ne the situation is quite different. A single strong $\Delta T=1$ transition is observed to the 1^+ level at 11.2 MeV, which is predominantly orbital as predicted by shell model calculations.[33] In $T_z=0$ nuclei like ^{20}Ne the strong $M1$ transitions must be isovector in accordance with the Morpurgo selection rule.[34] Consequently, only those analog states with $T=1$ will be excited. These analog states, which correspond to the low-lying states in the neighboring mirror nuclei, have very little $d_{3/2}$ amplitude in their wave functions. Consequently, the spin-flip contributions to the $M1$ matrix element will be small and the larger $d_{5/2}$ components in both the ground and excited state wave functions will dominate the $M1$ matrix element.

V. CONCLUSIONS

The total measured $M1$ strength in ^{22}Ne is more than one half of the value predicted by the sum rule and is consistent with the trend suggested by the extreme single particle model. The fragmentation of the $M1$ strength is predicted by the *sd* shell model[8] and the strength of the three strongest transitions are each within a factor of two of the predictions. The distribution of strength is similar to that in the $T=1$ nucleus ^{26}Mg, but much different from the concentration of strength observed in the $T=0$ nuclei ^{20}Ne, ^{24}Mg, and ^{28}Si.

ACKNOWLEDGMENTS

We thank Dr. B. H. Wildenthal for providing us with calculations of the reduced matrix elements. We also thank Professor H. Überall for his critical reading of the manuscript and stimulating discussions. Mr. R. Tobin and the Linac Staff is acknowledged for maintaining and operating the accelerator and for assistance in many other tasks. One of the authors (XKM) wishes to thank Dr. J. McElhinney and the Nuclear Sciences Division at Naval Research Laboratory for their hospitality during his three month stay.

*Naval Postgraduate School, Monterey, California.
†On leave from University of Rochester, Rochester, New York.

[1]L. W. Fagg, in *Proceedings of the International Conference on Photonuclear Reactions and Applications, Asilomar, 1973*, edited by B. L. Berman (Lawrence Livermore Laboratory, Univ. of California, Livermore, 1973), Vol. 2, p. 675.
[2]W. L. Bendel, L. W. Fagg, S. K. Numrich, E. C. Jones, Jr., and H. F. Kaiser, Phys. Rev. C 3, 1821 (1971).
[3]L. W. Fagg, W. L. Bendel, R. A. Tobin, and H. F. Kaiser, Phys. Rev. 171, 1250 (1968); and O. Titze, Z. Phys. 220, 66 (1969).
[4]L. W. Fagg, W. L. Bendel, E. C. Jones, Jr., and S. Numrich, Phys. Rev. 187, 1378 (1969).
[5]W. L. Bendel, L. W. Fagg, R. A. Tobin, and H. F. Kaiser, Phys. Rev. 173, 1103 (1968); and O. Titze and E. Spamer, Z. Naturforsch. 21a, 1504 (1966).
[6]B. M. Preedom and B. H. Wildenthal, Phys. Rev. C 6, 1633 (1972).
[7]D. Kurath, Phys. Rev. 130, 1525 (1963).
[8]B. H. Wildenthal, private communication.
[9]M. Rosen, R. Raphael, and H. Überall, Phys. Rev. 163, 927 (1967).
[10]B. T. Chertok, W. T. K. Johnson, and D. Sarkar, in *Table of Coulomb Distortion Corrections to Inelastic Electron Scattering Cross Sections for Magnetic-Dipole and Quadrupole Transitions* (The American University, Department of Physics, Washington, D.C., 1970).
[11]C. Toepffer and D. Drechsel, Z. Phys. 210, 423 (1968).
[12]See, for example, S. J. Skorka, J. Hertel, and T. W. Retz-Schmidt, Nucl. Data A 2, 347 (1966).
[13]P. K. A. de Witt Huberts, H. de Vries, G. J. C. van Niftrik, and G. A. Peterson, Nucl. Instrum. Methods 74, 27 (1969).
[14]L. W. Fagg, E. C. Jones, Jr., and W. L. Bendel, Nucl. Instrum. Methods 77, 136 (1970).
[15]L. Landau, J. Phys. USSR 8, 201 (1944).
[16]H. Bethe and W. Heitler, Proc. R. Soc. Lond. A146, 83 (1934).
[17]L. C. Maximon, Rev. Mod. Phys. 122, 193 (1969).
[18]C. de Vries, R. Hofstadter, A. Johansson, and R. Herman, Phys. Rev. 134, B848 (1966).
[19]F. Borkowski, P. Peuser, G. Simon, V. H. Walthe, and R. D. Wendling, in *Proceedings of the International Conference on Photonuclear Reactions and Applications, Asilomar, 1973* (see Ref. 1), Vol. 2, p. 889.
[20]R. H. Stokes and P. G. Young, Phys. Rev. 178, 1789 (1969).
[21]P. M. Endt and C. Van der Leun, Nucl. Phys. A214, 1 (1973), and references therein.
[22]M. G. Silbert and N. Jaramie, Phys. Rev. 123, 221 (1961).
[23]S. Hinds, private communication to Ref. 21.
[24]P. Neogy, R. Middleton, and W. Scholz, Phys. Rev. C 6, 885 (1972).
[25]W. Scholz, P. Neogy, K. Bethge, and R. Middleton, Phys. Rev. C 6, 893 (1972).
[26]W. Kutschera, D. Pelte, and G. Schrieder, Nucl. Phys. A111, 529 (1968).
[27]G. Chouraqui, Th. Muller, M. Port, and J. M. Thirion, J. Phys. (Paris) 31, 249 (1970).
[28]S. Gorodetzky, M. Port, J. Graff, J. M. Thirion, and G. Chouraqui, J. Phys. (Paris) 29, 271 (1968).
[29]J. B. French, E. C. Halbert, J. B. McGrory, and S. S. M. Wong, in *Advances in Nuclear Physics*, edited by M. Baranger and E. Vogt (Plenum, New York, 1969), Vol. 3.
[30]E. C. Halbert, J. B. McGrory, B. H. Wildenthal, and S. P. Pandya, in *Advances in Nuclear Physics*, edited by M. Baranger and E. Vogt (Plenum, New York, 1971), Vol. 4.
[31]T. T. S. Kuo, Nucl. Phys. A103, 71 (1967).
[32]S. Yoshida and L. Zamick, Annu. Rev. Nucl. Sci. 22, 121 (1972).
[33]S. Maripuu and B. H. Wildenthal, Phys. Lett. 38B, 464 (1972).
[34]G. Morpurgo, Phys. Rev. 110, 721 (1958).